DFT Study of the Metal Coordination Center Domain of Fe(II)−Bleomycin

Marek Freindorf and Pawel M. Kozlowski*

Department of Chemistry, University of Louisville, Louisville, Kentucky 40292

Received: January 31, 2001; In Final Form: May 17, 2001

We present a comprehensive analysis of the geometric and electronic properties of the metal coordination center domain of the iron(II) complex of the antitumor drug bleomycin (BLM) using density functional theory (DFT). The various experimental studies devoted to establishing the nature of the metal coordination center in BLM suggest that the metal is five-coordinated, with a sixth site available for exogenous ligand binding. Among the five ligands, four of them form an equatorial coordination sphere, but the nature of the fifth axial ligand remains controversial. To elucidate the nature of the metal coordination center in Fe(II)−BLM, six structurally different conformers resembling the active site have been investigated using DFT. An optimal geometry has been found for each conformer in the singlet, triplet, and quintet electronic states. The electronic ground state was identified as a four-coordinate species with intermediate spin state. However, when the results of these calculations were compared with the latest 2D NMR data, the best agreement was found between the five-coordinated theoretical model and experiment. Stereoelectronic analysis of four-coordinate conformers has shown that the Fe out-of-plane displacement controls the spin state. The high-spin state potential energy surface intersects the triplet state potential energy surface along the doming-mode coordinate when the iron atom is displaced about 0.4 Å from the equatorial nitrogens average plane. This intersection is the result of different iron d orbital occupancy in quintet and triplet electronic states.

Introduction

Bleomycins (BLMs, Figure 1), mononuclear nonheme iron complexes, are a group of glycopeptide antibiotics synthesized by *Streptomyces verticillus*[1,2] that are widely used in chemotherapy against some types of carcinoma.[3,4] The drug Blenoxane,[5−7] based on the bleomycins, is one of the most successful for anticancer treatment because of its ability to degrade duplex DNA,[8−11]and possibly RNA[12] selectively. It is generally accepted that DNA degradation is both oxygen and metal ion dependent with the greatest enhancement in vivo observed for iron.[13,14] Oxygen binds to high-spin Fe(II)−BLM to produce oxygenated O_2−Fe(II)−BLM[15,16] that is a precursor to the active species in the DNA cleavage mechanism. In this mechanism, the coordination chemistry of Fe(II)−BLM appears to play a key role in its unique oxygen chemistry and reactivity. The structure of Fe(II)−BLM has been intensively investigated using various bioanalytical and spectroscopic techniques;[17] however, the precise geometry of this complex is not yet known.

The aim of the present work is to provide theoretical insight into the ground state geometry and electronic structure of the metal coordination center of Fe(II)−BLM using density functional theory (DFT). To accomplish this, we propose a computationally feasible model of a metal coordination center together with several conformers which can be obtained from the proposed model. For each conformer, we present DFT calculations of low, intermediate, and high spin states to obtain a correlation between the ground-state geometry and electronic structure. Finally, we present a comparison with the latest 2D NMR data to establish a reliable model for the ground-state geometry and suggest possible implications for a mechanism of DNA cleavage.

* To whom correspondence should be addressed. E-mail: pawel@louisville.edu.

Model of Metal Coordination Center

The initial model for the expected coordination of metallo-BLM was derived from the X-ray structure of a Cu(II) complex of a biosynthetic precursor of BLM.[18] In this structure, the secondary amine of aminoalanine (A″−aALA), the pyrimidine (PYR), the histidine amide (HIS−A), and the histidine imidazole (HIS−I) are equatorial ligands, whereas the primary amine of aminoalanine (A′−aALA) is an axial ligand. Unfortunately, this complex lacks the sugar gulose (GUL), the mannose (MAN) residue and the bithiazole (BITH) tail. Early spectroscopic studies[19] suggested that the Fe(II)−BLM coordination center has a five-coordinate, square pyramidal geometry with A″−aALA, PYR, and HIS−I groups equatorially liganded to the central Fe(II) atom, but the identity of a fourth equatorial and an axial ligand remained in dispute. EPR studies[20] of nitrosyl ternary complexes of Fe(II)−BLM, suggested axial ligation of A′−aALA and equatorial ligation of deprotonated HIS−A of this early proposed structure. In contrast, NMR experiments[21,22] support an alternative coordination site of CO−Fe(II)−BLM or Zn(II)−BLM in which the equatorial HIS−I does not ligate; rather, the fourth equatorial site is occupied by A′−aALA with MAN as an axial ligand. Utilization of 2D NMR[23] techniques to CO−Fe(II)−BLM has led to a structure with A″−aALA, PYR, HIS−I, and HIS−A as equatorial ligands, in agreement with earlier studies, and MAN as an axial ligand. More recently, a NMR study[24] of Fe(II)−BLM supports an alternative structure where equatorial ligands are the same as above, but A′−aALA is placed as the coordination site axial ligand. Resonance Raman studies[25] of CO−Fe(II)−BLM suggested a structure where A″−aALA, PYR, HIS−A, and HIS−I are equatorial ligands and A′−aALA as an axial ligand. Finally, in recent spectroscopic investigations[28] of Fe(II)-BLM, a dynamic structure has been proposed where A′−aALA is a permanent axial ligand with A″−aALA, PYR, HIS−A, and HIS−I as equatorial ligands,

10.1021/jp010406d CCC: $20.00
Published on Web 06/29/2001

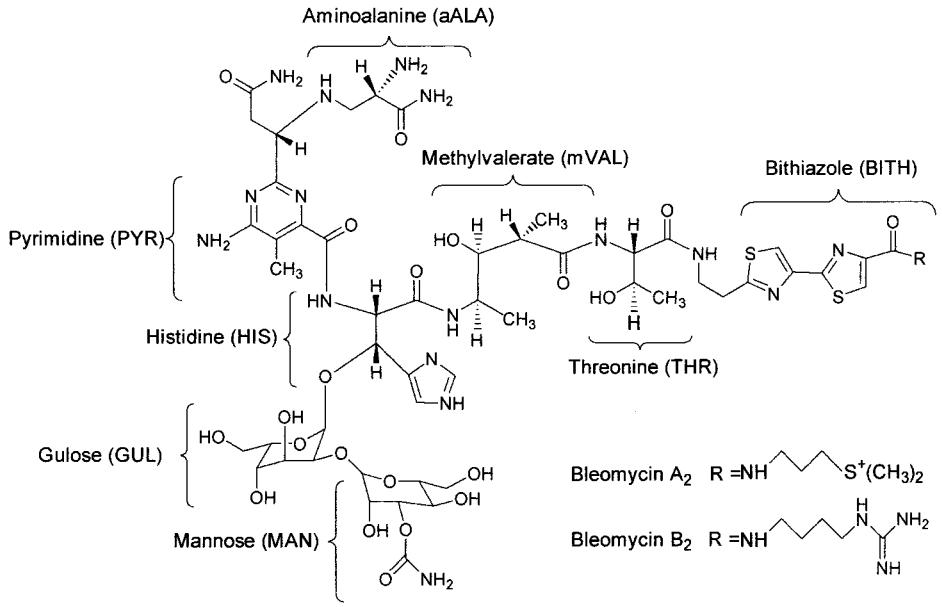

Figure 1. Molecular structure of bleomycins (BLMs).

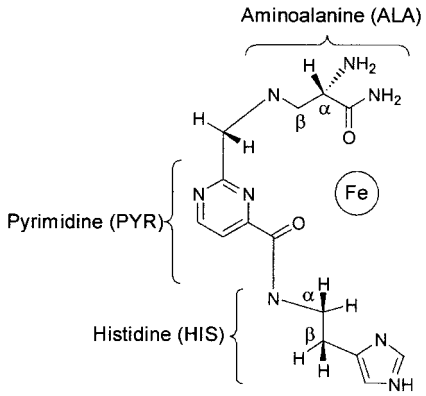

Figure 2. Model of the metal coordination center domain of Fe(II)−BLM.

but MAN weakly occupies the sixth binding site. Throughout these experimental investigations described above, there is unclear evidence supporting the position of the MAN residue in the coordination site of the complex; however, the predominant axial coordination of the A′−aALA residue is more strongly supported.

Fe(II)−BLM possesses four main structural domains including a bithiazole tail, a linker region, a metal binding domain, and a disaccharide moiety (Figure 1). To describe the coordination environment of the metal domain of the complex, we have investigated a simplified model which retains the important structural features (Figure 2). This computationally feasible model consists of the A″−aALA, PYR, HIS−A, and HIS−I residues as equatorial ligands of the Fe(II) center and the A′−aALA residue as a permanent axial ligand. In fact, several different possibilities have been tested by DFT calculations. All alternative arrangements of ligands lead to higher energies and tensions in the metal coordination sphere. The remaining parts of the Fe(II)−BLM complex are the bithiazole tail, a linker region, and a disaccharide moiety that have been excluded from the model compound for simplicity of computational calculations. In addition, a methyl group, a primary amine of PYR, and an amide group located between PYR and aALA residues have also been excluded from the model compound. The final model can exist in two different conformers with respect to the

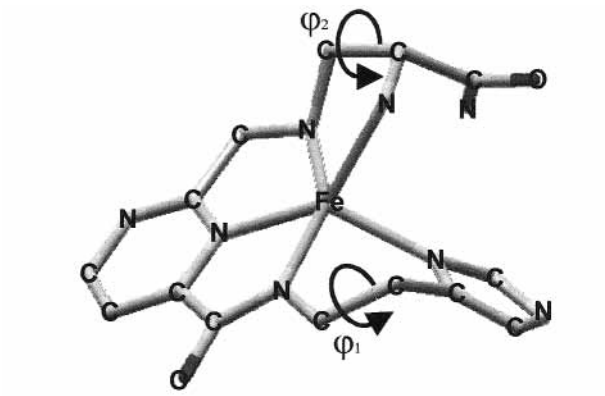

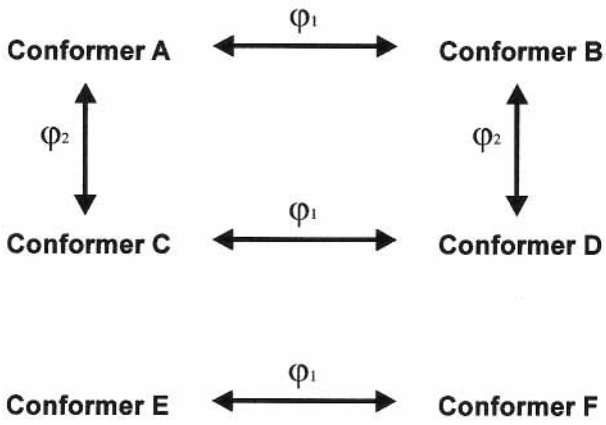

Figure 3. Structure of conformer A and its interconnections with other conformers through (φ_1, φ_2) tortional angles. The hydrogen atoms have been omitted for simplicity.

$C_\alpha-C_\beta$ bond (angle φ_1, Figure 3) of the HIS residue and two different conformers with respect to the $C_\alpha-C_\beta$ bond (angle φ_2, Figure 3) of the aALA residue. These five-coordinated conformers have been denoted as A, B, C, and D, respectively. Two additional conformers E and F have been created where the aALA residue was bent away from the metal center in order to describe the coordination site of the fourth coordinated metal center (Figure 3).

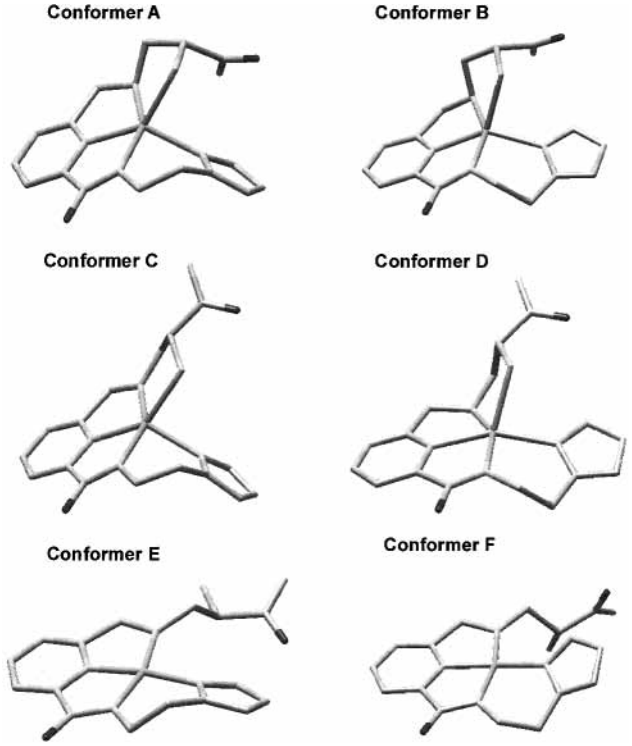

Figure 4. Optimized structures of the model complexes in their ground electronic states. The hydrogen atoms have been omitted for simplicity.

TABLE 1: Relative Energies of the Conformers in Different Electronic States

	energy (kcal/mol)[a]		
conformer	singlet	triplet	quintet
A	25.8	9.0	3.6
B	27.7	10.1	3.5
C	21.9	4.5	5.2
D	24.1	7.2	5.9
E	20.9	0.0	5.4
F	24.6	1.7	5.9

[a] The reference energy is the ground triplet electronic state energy of the conformer *E*, which has the value $E_{ref} = -2396.4936$ au.

Computational Details

DFT calculations reported in this work have been carried out using the B3LYP composite exchange-correlation functional and the 6−31G(d) basis set as implemented in the Gaussian 98[27] suite of programs. For each conformer under consideration, a full geometry optimization assuming low, intermediate, and high spin states has been performed. The final structures of the metal complexes are shown in Figure 4, whereas electronic energies corresponding to singlet, triplet, and quintet states of these complexes are summarized in Table 1. The most important geometric parameters, including metal−ligand bond lengths of the coordination sphere and out-of-plane iron displacement are presented in Table 2. The Supporting Information provides a list of all optimized coordinates.

Theoretical Analysis of Conformers

Several interesting conclusions can be made from the present DFT calculations: among all of the conformers under consideration, conformer E has the lowest energy in its triplet electronic state. In this complex, the metal center has a planar coordination sphere and the arm of the aALA residue is pointing away from the metal atom producing the planar hybridization of the A′−aALA nitrogen atom. In the final structure, conformer E has the imidazole ring of the HIS residue pointing away from the tail of the aALA residue, creating the structure with the smallest intermolecular interactions between these two residues. The electronic quintet state of conformer E lies about 5.4 kcal/mol above the ground triplet electronic state, whereas the singlet electronic state is located over 20.9 kcal/mol above the ground state. The average metal−ligand bond lengths vary monotonically with spin, being smallest in the singlet electronic state and largest in the quintet.

Conformer F was generated from conformer E by a change in the tetrahedral angle φ_1 around the $C_\alpha-C_\beta$ bond of the HIS residue. After geometry optimization, conformer F has the imidazole ring of the HIS residue pointing toward the arm of the aALA residue causing stronger steric interactions between these two groups than in the conformer E. These interactions cause the ground triplet electronic state of conformer F to be higher energetically by about 1.7 kcal/mol above the reference ground triplet electronic state of conformer E. Similarly, as in conformer E, conformer F has the quintet electronic state located about 5.9 kcal/mol and the singlet electronic state located about 24.6 kcal/mol higher than the reference state of conformer E. The change in the tetrahedral angle φ_1 around the $C_\alpha-C_\beta$ bond of the HIS residue from conformer E to conformer F does not influence the average length of the metal−ligand bond. The bond-length dependence on spin for conformer F mirrors that of conformer E discussed above.

Among the five-coordinated structures, conformers A and B have the lowest energy in their quintet electronic states. Conformer A was built from conformer E by attachment of the arm of the aALA residue to the metal center via the A′−aALA nitrogen atom, creating a fifth coordinated compound. In its ground quintet electronic state, this complex is located about 3.6 kcal/mol above the triplet ground electronic state of reference conformer E. The first excited electronic state of conformer A is a triplet located about 9.0 kcal/mol above the reference triplet state. The singlet electronic state is the next state of conformer A and lies about 25.8 kcal/mol above the reference state. In conformer A, the A″−aALA nitrogen atom has no planar hybridization and the equatorial ligands of the metal center are not as planar as the four coordinated structures E and F. The additional, axial A′−aALA ligand changes the coordination sphere of conformer A into a domed structure, but this effect does not influence the lengths of the equatorial metal bonds. The equatorial metal−ligand bonds of the conformer A are similar to those in conformer E; however, a new axial bond between the metal atom and the A′−aALA nitrogen atom is the longest in all electronic states. Moreover, the axial metal bond has the largest value in the triplet electronic state, whereas the mean equatorial metal bond is largest in the quintet state. The domed structure of conformer A is different in different states. In the singlet electronic state, the metal coordination is almost planar, whereas in the triplet electronic state, it becomes more nonplanar producing the most distorted structure in the quintet electronic state.

Similar to the four-coordinated complexes E and F, conformer B was generated from conformer A by changing the tetrahedral angle φ_1 around the $C_\alpha-C_\beta$ bond of the HIS residue. The ground electronic state of complex B is quintet and is located about 3.5 kcal/mol above the ground triplet electronic state of reference conformer E. The next electronic state of conformer B is a triplet state lying about 10.1 kcal/mol above the ground state, followed by the singlet state located about 27.7 kcal/mol. Having a different orientation of the HIS residue, conformer B still keeps the domed structure of the metal coordination center. Similar

TABLE 2: Metal−Ligand Bond Lengths and Fe out of Plane Displacements of the Conformers in Different Electronic States

	metal bond lengths (Å)								
	mean equatorial[a]			axial[b]			Fe out of plane displacements (Å)[c]		
conformer	singlet	triplet	quintet	singlet	triplet	quintet	singlet	triplet	quintet
A	1.97	1.97	2.12	1.99	2.32	2.29	0.14	0.14	0.33
B	1.98	1.97	2.13	1.99	2.31	2.27	0.12	0.12	0.23
C	1.95	1.94	2.11	1.98	2.34	2.28	0.11	0.11	0.24
D	1.96	1.94	2.11	1.97	2.31	2.29	0.08	0.08	0.16
E	1.89	1.93	2.05				0.03	0.03	0.07
F	1.89	1.94	2.05				0.09	0.01	0.11

[a] Arithmetic mean of the four bond lengths between the Fe atom and the equatorial N atoms. [b] The bond length between the Fe atom and the axial N ligand. [c] The difference between the Fe atom position and the arithmetic mean position of the equatorial N atoms.

TABLE 3: Comparison of the Theoretical and Experimental Fe−H Distances

	Fe−H distances (Å)						
	theoretical[a]						
assignments[b]	A	B	C	D	E	F	expt[c]
HIST $C^{\alpha}H$	3.96(0.36)	3.38(0.22)	3.92(0.32)	3.49(0.11)	3.92(0.32)	3.57(0.03)	3.6
1/2 ALA $C^{\beta}H_2$	3.96(0.14)	3.92(0.18)	3.91(0.19)	3.90(0.20)	3.79(0.31)	3.96(0.14)	4.1
PYR $C^{\beta}H$	3.86(0.76)	3.54(0.44)	3.73(0.63)	3.88(0.78)	3.61(0.51)	3.68(0.58)	3.1
ALA $C^{\alpha}H$	4.04(0.34)	4.01(0.31)	3.35(0.35)	3.59(0.11)	3.91(0.21)	3.17(0.53)	3.7
1/2 ALA $C^{\beta}H_2$	3.40(0.00)	3.12(0.28)	3.56(0.16)	3.14(0.26)	3.08(0.32)	3.36(0.04)	3.4
HIST C2H	3.54(0.44)	3.42(0.32)	3.53(0.43)	3.44(0.34)	3.32(0.22)	3.34(0.24)	3.1
HIST N3H	5.30	5.25	3.29	5.26	5.04	5.06	
HIST C4H	5.32(0.32)	5.39(0.39)	5.31(0.31)	5.38(0.38)	5.15(0.15)	5.17(0.17)	5.0
HIST $C^{\beta}H$	4.40(0.00)	3.73(0.67)	4.39(0.01)	3.60(0.80)	4.37(0.03)	3.37(0.03)	4.4

[a] Numbers in parantheses correspond to deviation between optimized and NMR-based distances. [b] Notation has been taken from ref 24. [c] Experimental data have been taken ref 24.

to complex A, the domed structure of the coordination sphere of complex B changes from the almost planar structure in the singlet electronic state to the most distorted structure in the quintet electronic state, having the intermediate conformation in the triplet electronic state. The four equatorial bonds of complex B are similar to those of complex A, as well as the axial metal bond having a similar length in both complexes A and B.

The next two conformers of the Fe(II)−BLM complex have the A′−aALA arm pointing away from the metal coordination plane keeping the bond between the A′−aALA nitrogen atom and the Fe metal center. Conformers C and D were generated from conformers A and B by changing the tetrahedral angle φ_2 around the $C_{\alpha}-C_{\beta}$ bond of the A′−aALA residue, respectively. The ground electronic state of conformer C is a triplet, and it lies about 4.5 kcal/mol higher than the triplet electronic ground state of reference complex E. The quintet state is located about 5.2 kcal/mol, whereas the singlet is located about 21.9 kcal/mol above the reference state. Similar to the other five-coordinated conformers, conformer C still keeps the domed structure of the metal coordination sphere. This structure changes from almost planar in the singlet electronic state, through the intermediate conformation in the triplet state, to the most distorted in the quintet electronic state. The four equatorial metal bonds and the axial metal bond have similar lengths to the other five-coordinated complexes.

The last complex D was generated from complex C in the same way as the other five-coordinated complexes by changing the tetrahedral angle φ_1 around the $C_{\alpha}-C_{\beta}$ bond of the HIS residue. The ground quintet electronic state of conformer D is located about 5.9 kcal/mol above the triplet ground state of reference conformer E. The triplet and the singlet states of this complex are placed about 7.2 and about 24.1 kcal/mol above the reference state, respectively. Similar to the other five-coordinated complexes, conformer D has the domed structure of the metal coordination sphere, which changes from planar in the singlet electronic state, through intermediate in the triplet state, to domed in the quintet state. The metal equatorial and axial bonds have similar values in complex D as in the other five-coordinated complexes.

Comparison with Experiment

The stereoelectronic analysis presented in the previous section suggests that a four-coordinated complex with intermediate spin state can be identified as the electronic ground state of the iron coordination center domain. It is therefore interesting to compare these results with the latest experimental data. Table 3 summarizes the comparison between the iron-proton DFT optimized distances for six investigated conformers compared with the Fe−H distances based on 2D NMR studies of the paramagnetic complex Fe(II)−BLM.[24] The experimental iron−proton distances were obtained from relaxation times of the paramagnetically behaved protons. According to these data, a discrepancy of 0.6−1.0 Å occurs for the Fe−H distances (HIS $C^{\beta}H$) for B, D, and F conformers. In these conformers, where the tetrahedral angle φ_1 is roughly similar, the HIS residue is pointing toward the aALA group and this geometry seems to be inconsistent with experiment. Among three other conformers A, C, and E, where the HIS residue is pointing away from the aALA group, conformer E has a discrepancy of 0.3 Å for the Fe−H distances (aALA $C^{\beta}H_2$) between DFT optimized and experimental data. This conformer has the aALA group bent away from the metal coordination center which is inconsistent with the experimental data. Both conformers A and C have comparable agreement of the experimental and theoretical Fe−H distances; however, they have different tetrahedral angles φ_2, which describes the position of the aALA residue. Conformer A has the aALA $C^{\alpha}H$ hydrogen pointing away from the metal coordination center having the longer Fe−H distance (ALA $C^{\alpha}H$) than this distance in conformer C where the aALA residue is pointing toward the Fe atom. Taking into account these small differences, which

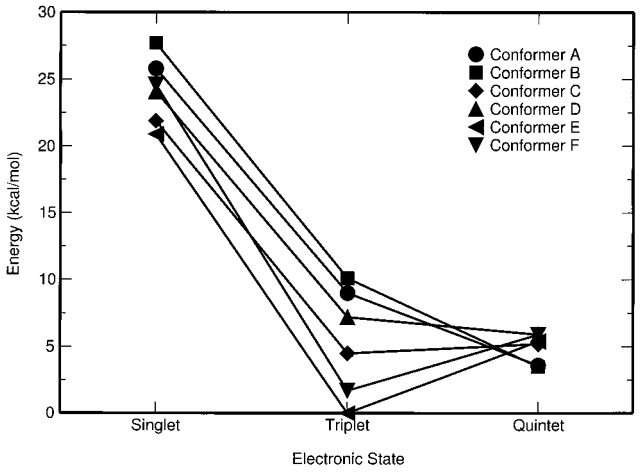

Figure 5. Relative energies of conformers in different electronic states.

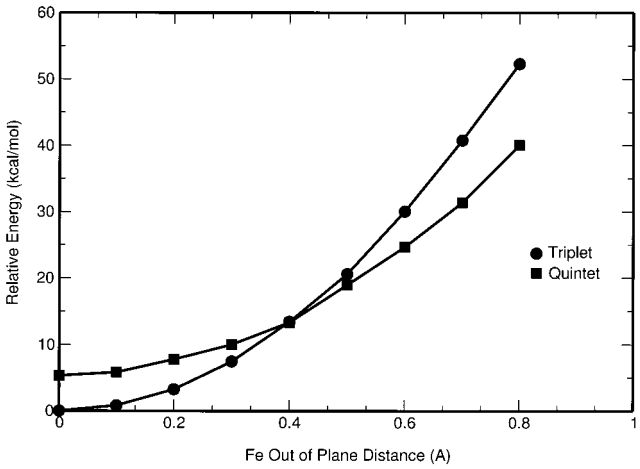

Figure 6. Relative energies of four-coodinated conformer E in the triplet and quintet electronic states calculated as the iron out of plane displacement.

are about 0.3 Å in both A and C conformers, it is difficult to judge which conformer more closely resembles the experimental structure. The final conclusion can be reached taking into account the energies of these two conformers: among the five-coordinated complexes conformer, A has the lowest energy in the quintet electronic state. This conformer corresponds to the structure which is the most frequently suggested in experimental investigations, where the axial coordination of the A′−aALA amine is strongly supported. In summary, the present DFT calculations reproduce well the relative positions of both HIS and A′−aALA residues in conformer A with respect to the central Fe atom.

Summary and Conclusions

In the absence of axial ligation, the iron complexes of BLM have intermediate spin, whereas the majority of five-coordinated species display high spin electronic states (Figure 5). Both four-coordinated conformers E and F have the triplet electronic ground state, whereas the lowest electronic states of the five-coordinated complexes A, B, and D are quintets. However, the energy difference of the ground electronic state between different conformers is only of the order of a few kcal/mol and the presence of the additional fifth ligand displaces the iron atom from the equatorial coordination plane changing the ground electronic state from triplet to quintet. Interestingly, the electronic state of four coordinated complexes is controlled by only one geometrical parameter, the iron out-of-plane displacement. To explain this effect, we carried out calculations on reference complex E in the quintet and triplet electronic states. In these calculations, the iron atom has been successively displaced out of the average nitrogen plane and relative energies calculated as a function of iron displacement (Figure 6). The energy corresponding to the iron out of plane iron displacement was obtained without geometry optimization. The relative electronic energies show that the ground state of model complex E is triplet when the metal is located in the plane of the four equatorial nitrogens and becomes quintet when the iron displacement is more than 0.4 Å. This effect can be attributed to different iron d orbital occupations in different electronic states. In the singlet electronic state, the d_{z^2} and $d_{x^2-y^2}$ iron orbitals are not occupied, whereas in the quintet electronic state, they are both singly occupied. In the triplet state, the d_{z^2} orbital is occupied, whereas $d_{x^2-y^2}$ is empty. The $d_{x^2-y^2}$ orbital becomes occupied in the high-spin state and is less antibonding when Fe is out of plane. Therefore, attaching the A′−ALA arm to the coordination sphere moves the Fe metal atom out from the coordination plane, changing the ground electronic state from triplet to quintet.

DFT calculations show that complexes A, C, and E, where the HIS residue is pointing away from the A′−aALA residue, have lower energies than the corresponding complexes B, D, and F in the corresponding electronic states. The interaction between the HIS and A′−aALA groups seems to play an important role in these systems. For five-coordinated complexes A, B, C, and D, the axial metal bond with the A′−aALA nitrogen atom has a bigger value than the average equatorial metal bond in the electronic states. The five-coordinated models A, B, C, and D show that the domed structure of the coordination sphere changes from almost planar in the singlet electronic state to the most distorted structure in the quintet electronic state, keeping the intermediate conformation in the triplet electronic state. The equatorial metal bond lengths are shortest in the singlet electronic states, longer in the triplet electronic state, and longest in the quintet electronic state.

Interestingly, the metal coordination center of BLM exhibits many similar stereoelectronic properties observed for metalloporphyrins. The four-coordinate iron porphyrins have an intermediate spin state, but when the iron is displaced approximately 0.4 Å out of the porphyrin plane (domed motion), the ground-state becomes high spin.[28−30] For iron porphyrins, the transition from intermediate to high spin state is associated with so-called core expansion. We observed the same effect for Fe−N bond lengths in the case of Fe(II)−BLM. All conformers become essentially degenerate in their electronic quintet electronic states (Figure 5) because the metal coordination center is more flexible in comparison with singlet or triplet states. Although, we found that the four-coordinated conformer with the intermediate spin state has the lowest ground electronic state, the best agreement in terms of geometrical parameters, we found for the five-coordinated high spin state. One may suggest that the metal coordination center can be the subject of small molecular strain, which energetically is not very costly, being about 3 kcal/mol. This small strain keeps the iron out of plane as has been often suggested for the iron−histidine linkage in heme proteins.[29,30] The nonrigidity of the metal coordination center in its high spin state may have significant consequences for molecular recognition and interaction with DNA in the process of double strand cleavage.

Acknowledgment. The authors thank Dr. G. Lamm and Prof. R. M. Buchanan for helpful discussions.

Supporting Information Available: A list of all optimized coordinates. This material is available free of charge via the Internet at http://pubs.acs.org.

References and Notes

(1) Umezawa, H.; Maeda, K.; Takeuchi, T.; Okami, Y. *J. Antibiot. (Tokyo) Ser. A* **1966**, *19*, 200.

(2) Umezawa, H.; Suhara, Y.; Takita, T.; Maeda, K. *J. Antibiot. (Tokyo) Ser. A* **1966**, *19*, 210.

(3) Umezawa, H. In *Bleomycin*; Hecht, S. M., Ed.; Springer-Verlag: New York, 1979; p 24.

(4) Lazo, J. S.; Sebti, S. M. In *Anticancer Drug Resistance*; Kessel, D., Ed.; CRC Press: Boca Raton, FL, 1989; p 267.

(5) Crooke, S. T.; Brander, W. T. *J. Med.* **1976**, *7*, 333.

(6) Bajetta, E.; Rovej, R.; Buzzoni, R.; Vaglini, M.; Bonadonna, G. *Cancer Treat. Rep.* **1982**, *66*, 1299.

(7) Perry, D. J.; Weltz, M. D.; Brown, A. J., Jr.; Henderson, R.; Neglia, W. J.; Berenberg, J. L. *Cancer* **1982**, *50*, 2557.

(8) Stubbe, J.; Kozarich, J. W.; Wu, W.; Vanderwall, D. E. *Acc. Chem. Res.* **1996**, *29*, 322.

(9) Nagai, N.; Yamaki, H.; Suzuki, H.; Tanaka, N.; Umezawa, H. *Biochim. Biophys. Acta* **1969**, *179*, 165.

(10) Povirk, L. F.; Wubker, W.; Kohnlein, W.; Hutchinson, F. *Nucleic Acids Rev.* **1977**, *4*, 3573.

(11) Dedon, P. C.; Goldberg, I. H. *Chem. Res. Toxicol.* **1992**, *5*, 311.

(12) Hecht, S. M. *Bioconjugate Chem.* **1994**, *5*, 513.

(13) Absalon, M. J.; Kozarich, J. W.; Stubbe, J. *Biochemistry* **1995**, *34*, 2065.

(14) Absalon, M. J.; Wu, W.; Kozarich, J. W.; Stubbe, J. *Biochemistry* **1995**, *34*, 2076.

(15) Albertini, J. P.; Garnier-Suillerot, A.; Tosi, L. *Biochem. Biophys. Res. Commun.* **1982**, *104*, 557.

(16) Burger, R. M.; Kent, T. A.; Horwitz, S. B.; Munck, E.; Peisach, J. *J. Biol. Chem.* **1983**, *258*, 1559.

(17) Stubbe, J.; Kozarich, J. W. *Chem. Rev.* **1987**, *87*, 1107.

(18) Itaka, Y.; Nakamura, H.; Nakatani, T.; Muraoka, Y.; Fujii, A.; Takita, T.; Umezawa, H. *J. Antibiot.* **1978**, *31*, 1070.

(19) Stubbe, J.; Kozarich, J. W. *Chem. Rev.* **1987**, *87*, 1107.

(20) Sugiura, Y. *J. Am. Chem. Soc.* **1980**, *102*, 5208.

(21) Oppenheimer, N. J.; Rodriguez, L. O.; Hecht, S. M. *Proc. Natl. Acad. Sci. U.S.A.* **1979**, *76*, 5616.

(22) Oppenheimer, L. O.; Chang, C.; Chang, L. H.; Ehrenfeld, G.; Rodriguez, L. O.; Hecht, S. M. *J. Biol. Chem.* **1982**, *257*, 1606.

(23) Akkerman, M. A. J.; Neijman, E. W. J. F.; Wijmenga, S. S.; Hilbers, C. W.; Bermel, W. *J. Am. Chem. Soc.* **1990**, *112*, 7462.

(24) Lehmann, T. E.; Ming, L. J.; Rosen, M. E.; Que, L., Jr. *Biochemistry* **1997**, *36*, 2807.

(25) Takahashi, S.; Sam, J. W.; Peisach, J.; Rousseau, D. L. *J. Am. Chem. Soc.* **1994**, *116*, 4408.

(26) Loeb, K. E.; Zaleski, J. M.; Hess, C.; Hecht, S. M.; Solomon, E. I. *J. Am. Chem. Soc.* **1998**, *120*, 1249.

(27) Frisch, M. J.; Trucks, G. W.; Schlegel, H. B.; Scuseria, G. E.; Robb, M. A.; Cheeseman, J. R.; Zakrzewski, V. G.; Montgomery, J. A., Jr.; Stratmann, R. E.; Burant, J. C.; Dapprich, S.; Millam, J. M.; Daniels, A. D.; Kudin, K. N.; Strain, M. C.; Farkas, O.; Tomasi, J.; Barone, V.; Cossi, M.; Cammi, R.; Mennucci, B.; Pomelli, C.; Adamo, C.; Clifford, S.; Ochterski, J.; Petersson, G. A.; Ayala, P. Y.; Cui, Q.; Morokuma, K.; Malick, D. K.; Rabuck, A. D.; Raghavachari, K.; Foresman, J. B.; Cioslowski, J.; Ortiz, J. V.; Stefanov, B. B.; Liu, G.; Liashenko, A.; Piskorz, P.; Komaromi, I.; Gomperts, R.; Martin, R. L.; Fox, D. J.; Keith, T.; Al-Laham, M. A.; Peng, C. Y.; Nanayakkara, A.; Gonzalez, C.; Challacombe, M.; Gill, P. M. W.; Johnson, B. G.; Chen, W.; Wong, M. W.; Andres, J. L.; Head-Gordon, M.; Replogle, E. S.; Pople, J. A. *Gaussian 98*; Gaussian, Inc.: Pittsburgh, PA, 1998.

(28) Kozlowski, P. M.; Spiro, T. G.; Berces, A.; Zgierski, M. Z. *J. Phys. Chem. B* **1998**, *102*, 2603.

(29) Spiro, T. G.; Kozlowski, P. M.; Zgierski, M. Z. *J. Raman Spectrosc.* **1998**, *29*, 869.

(30) Kozlowski, P. M.; Spiro, T. G.; Zgierski, M. Z. *J. Phys. Chem. B* **2000**, *104*, 10659.